MULTI-SCALE ANALYSIS OF AN ILMENITE MICROCRATER IN LUNAR SAMPLE 71055.

B. A. Cymes[1], S. K. Noble[2], R. Christoffersen[1], T. Erickson[1], and L. P. Keller[3], [1]Jacobs, NASA Johnson Space Center, Mail Code XI3, Houston, TX 77058, USA (brittany.a.cymes@nasa.gov), [2]NASA Headquarters, 200 E St SW, Washington, DC 20546, USA, [3]NASA Johnson Space Center, Mail Code XI3, Houston, TX 77058, USA

Introduction: Micrometeorite impacts are a key space weathering process on the lunar surface, generating a variety of physical and chemical changes in the lunar regolith. [1]. Several experiments using nanosecond pulsed lasers to simulate micrometeorite impact have been published in the past two decades, providing a wealth of knowledge, including how minerals vary in their response to laser irradiation [e.g., 2-6]. Although these experiments have produced many features analogous to those observed in natural samples, none could be attributed to the passage of a shock wave, resulting instead from hot ablation [7]. Recent femtosecond laser irradiation of olivine and enstatite have more accurately reproduced the shock textures observed in lunar samples, improving our ability to coordinate experimental and lunar sample data [7-8].

Both pulsed laser experiments and studies of lunar impact craters [9] have focused on silicates, as they comprise the bulk of the regolith. Ilmenite ($FeTiO_3$) is the most abundant opaque mineral in lunar rocks [10] and an important sink of solar wind implanted helium [11]. Ilmenite is known to vary in its response to radiation processing relative to the silicates [12-13], but its response to micrometeorite impact has not yet been studied in natural samples nor in the laboratory. In this investigation, we characterize an ilmenite microcrater using scanning electron microscopy (SEM) and transmission electron microscopy (TEM) to learn how ilmenite responds to impact and if there are implications for helium cycling in the regolith.

Methodology: A microcrater in an ilmenite grain was identified on the surface of a 4.417 g piece of lunar sample 71055 and characterized by secondary electron and backscattered electron (BSE) imaging (Fig. 1a), and energy dispersive spectroscopy (EDS) mapping using a JEOL 7900F scanning electron microscope equipped with an Oxford 170 mm^2 SDD spectrometer. Transmitted Kikuchi diffraction (TKD) data were collected using an Oxford Symmetry electron backscattered diffraction system. A 30×20×0.1 µm cross-section of the microcrater was prepared for analysis using a FEI Quanta 3D Dual Beam focused ion beam (FIB)-SEM.

The cross-section was analyzed using a JEOL JEM-2500SE TEM/STEM operated at 200 keV. Imaging was performed in bright field (BF)-TEM, BF-STEM, dark field (DF)-STEM, and HAADF-STEM modes and STEM-EDS data were acquired using a JEOL 60mm^2 SDD spectrometer. Selected area electron diffraction (SAED) data were also collected.

Results: We identified a 15 µm crater on the surface of an ilmenite grain with a spall zone extending 5-10 µm beyond the rim (Fig. 1a). The crater cavity is coated with melt, splashing into and beyond the spall zone. The cross-section shows brittle and ductile shock deformation textures consisting of radial fractures, twins, and dislocations, the latter likely forming by basal slip on the (001) plane. The crater cavity stratigraphy consists of a ~10 nm Si-rich vapor deposit underlain by ~70 nm of solar wind damaged ilmenite, ~400 nm of ≥0.5 µm randomly oriented recrystallized melt domains, ~500 nm of ≤70 nm recrystallized melt domains fining downward, ~600 nm amorphous layer, and polycrystalline material extending ~1.5 µm deep (Fig. 1d). Beneath the polycrystalline layer is the highly deformed primary ilmenite crystal.

The lower two-thirds of the solar wind-damaged rim is deformed ilmenite structurally continuous with the underlying recrystallized layer, with no systematic depletion of Fe, Ti, or O relative to the underlying layer. The upper third of the solar wind-damaged layer contains <10 nm vesicular and non-vesicular opaques, and irregular to planar vesicles, (Fig. 2a), with increases in Fe and Ti relative to O (Fig. 2b) as compared to the underlying rim region. Anticorrelation of Fe and O and high-resolution images indicate that the opaques are $npFe^0$ (Fig. 2c). Other regions of the rim contain only vesicles in an amorphous Fe-depleted matrix adjacent to large elongate Fe^0 inclusions perpendicular to and breaching the surface. The surface of the spall zone has a thicker ~150 nm rim of $npFe^0$ and v-$npFe^0$ in a Ti-rich matrix overlain by a Si-rich vapor deposit.

Discussion: The microcrater cavities of plagioclase and pyroxene have been shown to contain glass melt overlying brittle-deformed substrates whereas olivine develops a recrystallized zone coarsening upward between a glass melt and a brittle-deformed substrate [9]. In comparison, the stratigraphy of the ilmenite crater cavity is more complex, with a fully amorphous layer sandwiched between the recrystallized layer above and the polycrystalline layer below. Ilmenite shows evidence of both brittle (fractures and polycrystallinity) and ductile (dislocations and twinning) deformation, in contrast to the silicates. However, because the size and density of the impactors are unknown, our ability to directly compare the data between these phases are

limited, necessitating more sampling.

Regarding the space weathered rim, our results are consistent with prior reports of ilmenite developing multiple distinct layers [12-15]: a Si-rich vapor deposit overlying a layer containing npFe^0 and planar vesicles overlying a defect-rich ilmenite structurally continuous with the underlying substrate. The planar vesicles here have some mutual orientation relative to the surface, though this varies in different recrystallized domains across the surface. Helium is known to be stored in planar vesicles on (001) in ilmenite [13]. Further investigation of the crystallographic orientation of the recrystallized domains relative to the vesicle orientations may reveal some additional relationships.

We observed the depletion in Fe in the space weathered rims of ilmenite reported previously [12-14], but only in areas where there were local elongate Fe^0 inclusions, all Fe having presumably migrated to form them during post impact recrystallization. It is unclear why certain areas of the rim developed these inclusions while others developed npFe^0, but it may be related to location variations in temperature during cooling.

Conclusion: We analyzed the microstructure and chemistry of a 15 µm crater from lunar sample 71055. Our results demonstrate that ilmenite responds differently to shock than olivine, plagioclase, and pyroxene by exhibiting distinct layers of vaporized, irradiated, recrystallized, and amorphous layers underlain by both brittle and ductile deformation textures. The solar wind-damaged layer shows irregular and planar vesicles and lateral variability in Fe^0 distribution and texture. These results point to meaningful variations in shock response among mineral phases that may have implications for the evolution and storage of volatiles in the regolith.

Acknowledgments: This work was supported by the Coordinated Analysis Work Package funded by NASA's Internal Scientist Funding Model (ISFM).

References: [1] Keller & McKay (1997) *GCA*, 61(11), 2331-2341. [2] Weber et al., (2020) *EPSL*, 530, 115884. [3] Loeffler et al., (2016) *MAPS*, 51(2), 261-275. [4] Brunetto et al., (2006) *Icarus*, 180, 546-554. [5] Sasaki et al., (2001) *Nature*, 410, 555-557. [6] Yamada et al., (1999) *Earth Planets Space*, 51, 1255-1265. [7] Fazio et al., (2018) *Icarus*, 299, 240-252. [8] Schmidt et al., (2018) *EPSC Abst.* 12, 284. [9] Noble et al. (2016) *LPS XLVII*, 1465. [10] Taylor (1992) *2nd Conf. Lunar Bas. Space Act. 21st Cent.*, 2. [11] Signer et al., (1977) *8th Proc. Lunar Sci. Conf.*, 3657-3683. [12] Christoffersen et al., (1996) *MAPS*, 31, 835-848. [13] Burgess & Stroud (2018) *GCA*, 224, 64-79. [14] Bernatowicz et al. (1994), *LPSC XXV*, 105-106. [15] Gu et al., (2022) Geophys. Res. Let., 49(7), e2022GL097875.

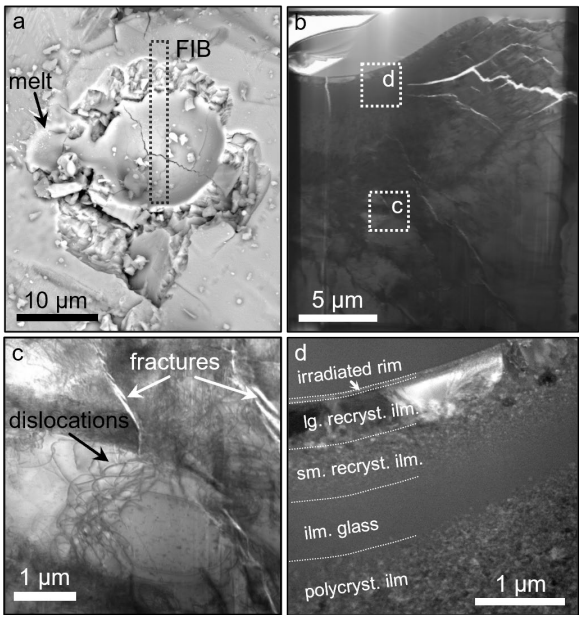

Fig. 1. The ilmenite microcrater analyzed in this study. (a) BSE image of the crater showing where the cross-section was extracted and the presence of melt lining the crater. **(b)** BF-STEM image of the prepared cross-section. **(c)** Inset of (b) showing detail of radial fractures and dislocations. **(d)** Inset of (b) showing detail of the crater cavity stratigraphy.

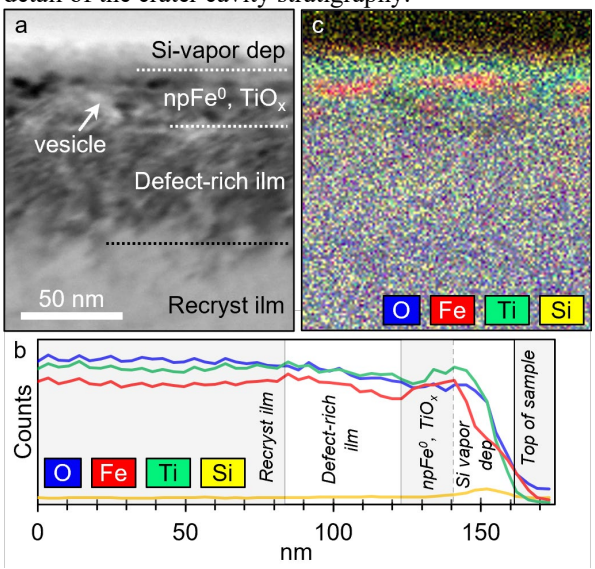

Fig. 2. Chemistry of the irradiated rim lining the crater cavity. (a) BF STEM image of the irradiated rim in the crater cavity. **(b)** Composite EDS element map of (a) showing distribution of O, Fe, Ti, and Si. **(c)** A 175 nm line scan from the interior of the rim to the surface showing counts of O, Fe, Ti, and Si with points extracted every 3 nm.